Interaction between Adatom-Induced Localized States and a Quasi-Two-Dimensional Electron Gas

Canhua Liu,* Iwao Matsuda, Rei Hobara, and Shuji Hasegawa
Department of Physics, School of Science, University of Tokyo, 7-3-1 Hongo, Bunkyo-ku, Tokyo 113-0033, Japan

(Received 29 September 2005; published 25 January 2006)

Using angle-resolved photoemission spectroscopy, we investigate changes in the band dispersion of a free-electron-like surface state of Si(111)-$\sqrt{3} \times \sqrt{3}$-Ag, induced by adsorption of submonolayer Au adatoms. At room temperature, where the adatoms are in a two-dimensional adatom-gas phase, electrons are transferred from the Au adatoms to the substrate, shifting the surface band downwards and causing it to deviate from a parabolic dispersion. At 135 K where the Au adatoms are frozen at specific sites of the substrate, the band splits into two. This band splitting can be explained in terms of hybridization between the unperturbed surface band and the localized virtual bound states induced by the Au adatoms.

DOI: 10.1103/PhysRevLett.96.036803 PACS numbers: 73.20.Hb, 71.10.Ca, 73.20.At

Crystal surfaces have surface electronic states that are trapped between the surface barrier potential toward a vacuum on one side and a band gap in the bulk states on the other side. These states are an empirical realization of a quasi-two-dimensional electron gas (2DEG), which has been a very good platform for studying impurity-induced phenomena. Theory states that any purely attractive potential always has at least one bound state in two dimensions [1]. Recently, such bound states localized around adatoms on metal surfaces have been detected by scanning tunneling microscopy or spectroscopy (STM or STS), for example, in the systems of Cu or Co adatoms on Cu(111) and Ag or Co on Ag(111) [2,3]. The existence of these bound states is a direct consequence of the 2D nature of surface states and the attractive potential induced by the adsorbates [2]. It has been suggested that a bound state is produced regardless of the type of adsorbates, and its hybridization with the surface band modifies the spectroscopic signature of the bound state [3] as well as the surface-state band itself. However, this phenomenon has not been demonstrated yet. Such an interaction between an extended state and a localized state has been a subject of great interest in revealing some very general physics applicable to various phenomena.

The surface of Si(111)-$\sqrt{3} \times \sqrt{3}$-Ag (hereafter, $\sqrt{3}$-Ag) has a 2DEG with a nearly free electron surface band that disperses at the Fermi level (E_F) [4]. Deposition of monovalent noble (Ag, Cu) or alkali (Na, K, Rb, Cs) atoms on $\sqrt{3}$-Ag induces a metallic 2D superstructure with a $\sqrt{21} \times \sqrt{21}$ period [5,6]. However, when the adatom coverage is much less than the saturation coverage, 0.142 monolayer [ML, where 1 ML equals 7.8×10^{14} cm^{-2}, the density of the topmost Si atoms in the ideal Si(111)1×1 surface], the adatoms distribute randomly on $\sqrt{3}$-Ag [7–9], which may induce a localized state similar to those on the metal surfaces mentioned above. Thus, a $\sqrt{3}$-Ag system with a small amount of monovalent adsorbates may be a good subject for observing the modification of surface states due to hybridization with localized states.

It is known, furthermore, that the behavior of monovalent adatoms on the $\sqrt{3}$-Ag surface depends on temperature. Previous STM studies of Ag and Cs adatoms [7,9] and the present study of Au adatoms [Fig. 1(a)] have shown that, at room temperature (RT), no adatoms appear in the STM images because they migrate rapidly on $\sqrt{3}$-Ag and form a 2D adatom-gas phase. At sufficiently low temperature (e.g., ~65 K) [Fig. 1(b)], the adatoms lose their diffusion mobility and stably reside at certain sites of the $\sqrt{3}$-Ag substrate. This property makes it possible to study the effect of adatoms on the 2DEG of the $\sqrt{3}$-Ag substrate by comparing the surface band at different temperatures.

In this Letter, we present angle-resolved photoemission spectroscopy (ARPES) measurements near E_F on $\sqrt{3}$-Ag with small amounts of Au adatoms deposited thereon. We show that the surface band has different features at RT and 135 K, due to the different states of the Au adatoms. The band splits in two at 135 K, while it remains singular at RT. This splitting can be explained in terms of hybridization between the unperturbed surface band and the Au adatom-induced localized states. At RT, on the other hand, the surface-band dispersion becomes nonparabolic with the adsorption of Au adatoms, which is shown by $\mathbf{k} \cdot \mathbf{p}$ per-

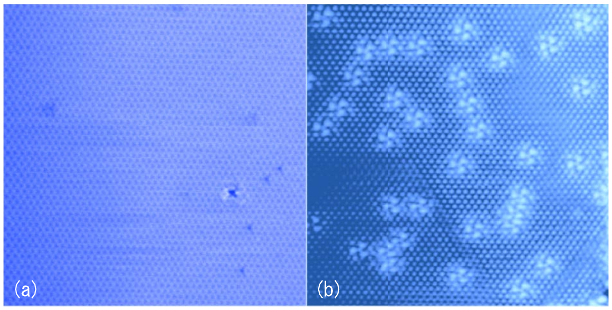

FIG. 1 (color online). Topographic STM images (31.2×31.2 nm^2) of the $\sqrt{3}$-Ag surface with 0.02 ML of Au adatoms thereon, taken at (a) RT ($V_{\text{tip}} = 1.80$ V, $I = 0.75$ nA) and (b) 65 K ($V_{\text{tip}} = -0.50$ V, $I = 0.75$ nA).

turbation theory to be due to hybridization with other surface states. This is the first observation of modulation in energy-band dispersion induced by the interaction between localized states and extended surface states.

The experiments were performed in a UHV chamber with a base pressure of $\sim 1 \times 10^{-10}$ Torr. The $\sqrt{3}$-Ag sample was produced by depositing 1 ML of Ag onto a Si(111)-7×7 clean surface at $\sim 520\,^\circ$C. Au was deposited onto the $\sqrt{3}$-Ag at RT. The Au coverage was calibrated by reflection high-energy electron diffraction by making a sequence of Au/Si(111) phases at optimal coverage [10]: 5×2 (0.44 ML), α-$\sqrt{3} \times \sqrt{3}$ (2/3 ML), and β-$\sqrt{3} \times \sqrt{3}$ phases (1 ML). In the ARPES measurements, the light source was He I with a photon energy of 21.2 eV and the analyzer was a Scienta SES-100 with an energy resolution of ~ 35 meV.

Figure 2 shows the ARPES results taken at (a)–(d) RT and (e)–(h) 135 K for various amounts of Au deposition on $\sqrt{3}$-Ag. The most significant feature is that the 2DEG band at RT splits in two bands at 135 K. Before discussing this main finding, we consider two important and useful issues that arise from the results at RT.

The first issue is the downward shift of the 2DEG band towards higher binding energies as the Au coverage increases. This can be explained by electron transfer from the Au adatoms to the $\sqrt{3}$-Ag substrate, as in the case of Ag adsorption [11]. The 2DEG Fermi wave vectors k_F taken from Figs. 2(a)–2(c) are 0.066, 0.093, and 0.113 Å^{-1} for Au coverages of 0.01, 0.02, and 0.03 ML, respectively. Thus, since the surface band is known to be isotropic [4], the number of electrons in this band can be calculated to be $k_F^2/2\pi = 6.93 \times 10^{16}\ e/\mathrm{m}^2$, $1.38 \times 10^{17}\ e/\mathrm{m}^2$, and $2.03 \times 10^{17}\ e/\mathrm{m}^2$, corresponding to Au coverages of 0.01, 0.02, and 0.03 ML, respectively. This indicates that each Au adatom transfers one electron to the 2DEG band, becoming a cation on the $\sqrt{3}$-Ag surface and producing an attractive potential for electrons around each Au adatom.

Besides the 2DEG band (usually called the S_1 band), the $\sqrt{3}$-Ag surface has two other surface bands, S_2 and S_3, at binding energies around 1 eV (not shown in Fig. 2) [5,6]. It is worth noting that the S_2 and S_3 bands exhibit no energy shift with the adsorption of Au adatoms [12], indicating that the rigid-band model for the $\sqrt{3}$-Ag surface breaks down [13].

The second important issue is that the dispersion of the S_1 band deviates from a parabola as the band shifts downwards. This is because the interaction between the S_2 and S_3 states and the S_1 state increases as the separation between them decreases due to the downward shift of the S_1 state. In this case the simple nearly free electron model is not appropriate and we have to use another approximation to depict the S_1 band. A first-principles calculation and STS measurements show that the S_1 state derives mainly from the Ag p_x and p_y orbitals, while the S_2 and S_3 states consist mainly of Ag $5s$ orbitals with some Ag $5p$ contributions [14]. Thus, $\mathbf{k} \cdot \mathbf{p}$ perturbation theory with the Kane

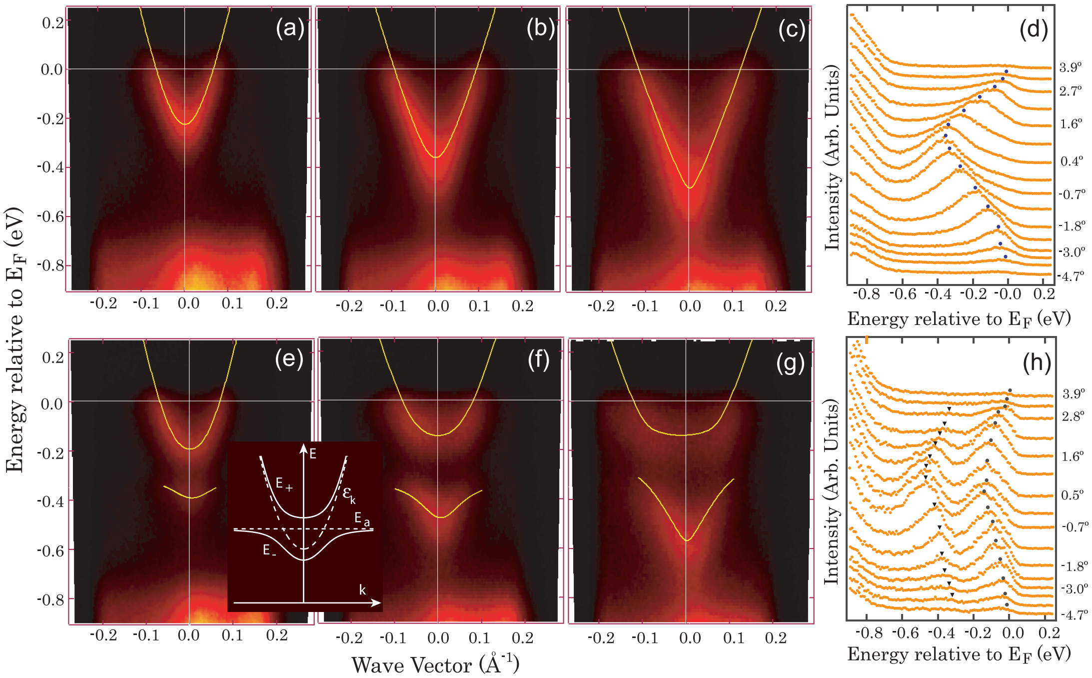

FIG. 2 (color online). Band dispersion of $\sqrt{3}$-Ag at (a)–(d) RT and (e)–(h) 135 K for Au adsorption at various coverages: (a),(e) 0.01 ML, (b),(f) 0.02 ML, and (c),(g) 0.03 ML. The origin of the wave vector is the second $\bar{\Gamma}$ point of the $\sqrt{3} \times \sqrt{3}$ surface Brillouin zone ($k = 1.09$ Å^{-1} in the direction $[10\bar{1}]$). The solid lines are fitted results by Eq. (1) [(a)–(c)] and Eq. (3) [(e)–(g)]. Panels (d) and (h) show parts of the raw spectra of (b) and (f), respectively. The inset between (e) and (f) is a schematic illustration of the hybridization between a conduction band and a localized virtual bound state.

model, which explains the bands of semiconductors consisting of s and p orbitals, may be a good method to describe these surface states approximately [15]. Following the Kane model, without the spin-orbit interaction for simplicity, we use the s-like and degenerate p-like orbital wave functions, $u_s(\mathbf{r})$ and $u_j(\mathbf{r})$ $(j = x, y)$, as the unperturbed basis set, and obtain the dispersion formula for the S_1 band by a degenerate perturbation theory calculation:

$$E(\mathbf{k}_\parallel) = E_s - \frac{E_g}{2} + \frac{\hbar^2 k_\parallel^2}{2m_0} + \left[\left(\frac{E_g}{2}\right)^2 + \frac{E_g \hbar^2 k_\parallel^2}{2m^*}\right]^{1/2}, \quad (1)$$

where $E_g = E_s - E_p$, with E_s and E_p the unperturbed energies of the s and p orbitals at $\mathbf{k} = 0$, respectively. m_0 is the free electron mass and $m^* = \hbar^2 E_g / 2|P|^2$, with $P = -(i\hbar/m_0)\langle u_s|\hat{\mathbf{p}}_j|u_j\rangle$.

For a pristine $\sqrt{3}$-Ag surface, the energy separation E_g between the S_1 band and the S_2 and S_3 bands is large enough that Eq. (1) can be simplified to the nearly free electron model. However, when the S_1 band shifts downwards, the dispersion $E(\mathbf{k}_\parallel)$ becomes similar to E_g as $\mathbf{k}_\parallel$ increases from $\bar{\Gamma}$. Hence the simplification is no longer valid. Instead we use Eq. (1) to reproduce the shifted S_1 band, as shown by the solid lines in Figs. 2(a)–2(c). The corresponding fitting parameters for each Au coverage are listed in Table I. These values are very credible, as we see that E_s indicates exactly the bottom of the S_1 band and the trends of E_g and m^* with Au coverage agree well with the observations.

We now return to discussing the splitting of the S_1 band at 135 K. The other bands, S_2 and S_3, show no change at 135 K. This splitting of the S_1 band is not only caused by Au adatoms but also by other monovalent metals, such as Ag and Cs deposited on the $\sqrt{3}$-Ag at 135 K, as shown in Fig. 3. Compared with the Au case, the Ag and Cs adatoms are not as stable on $\sqrt{3}$-Ag at 135 K and continue to migrate with a low mobility, which may be the reason why the splitting in Fig. 3 is not as clear as that in Fig. 2(h). Figure 3(a) was obtained for Ag adatoms deposited on the $\sqrt{3}$-Ag surface after it had been cooled to 135 K, for which 2D clusters of Ag adatoms formed on the surface, as shown by STM images [9]. However, when the sample was cooled down to 135 K after Ag was deposited on the surface at RT, the S_1 band did not split (not shown here) because the Ag adatoms aggregated into 3D microcrystals after deposition at RT [11] and the adatoms were not observed by STM at 135 K. This provides clear evidence that the band splitting is due to randomly dispersed adatoms that have been frozen at well-defined lattice sites and present a significant perturbation of the potential landscape of the bare $\sqrt{3}$-Ag surface.

TABLE I. Parameters for Eqs. (1) and (3) used to fit the bands in Fig. 2 at RT and 135 K, respectively.

Coverage	m^*/m_0	E_s (eV)	E_g (eV)	E_a (eV)	V (eV)
0.01 ML	0.064(5)	−0.22(3)	0.90(4)	−0.21(3)	0.11(2)
0.02 ML	0.054(4)	−0.36(1)	0.35(5)	−0.26(5)	0.13(1)
0.03 ML	0.023(3)	−0.48(1)	0.10(2)	−0.19(3)	0.12(3)

Recently, Crain *et al.* have also reported the opening of a similar gap in the S_1 band of $\sqrt{3}$-Ag with a small amount of Ag evaporated at low temperature [13]. However, they mainly concentrated on electron doping and made only a qualitative discussion of the gap, attributing it to a defect state associated with the Ag impurities. We present here a quantitative analysis of the band splitting to clarify the interpretation.

In a similar way to metal adatoms on a metal surface [2,3] or impurities in space charge layers of semiconductors [16], Au adatoms on a $\sqrt{3}$-Ag surface may induce bound states around them. The wave functions of these states overlap with each other at high enough concentrations and produce impurity bands whose dispersion is usually very small. In the case of Na^+ impurities in a semiconductor inversion layer, as a comparison, the Na concentration that gives rise to such an impurity band varies between about 10^{11} and 2×10^{12} cm^{-2} [16]. Since in the present case the Au coverage is about 1 to 3 times 7.8×10^{12} cm^{-2}, it is not surprising that such an impurity-like band results from the Au adatom-induced states. When the adatom-induced band crosses the 2DEG band of the $\sqrt{3}$-Ag substrate, the adatom-induced band becomes a resonant state and hybridizes with the 2DEG band, resulting in the splitting of the 2DEG band.

At RT, however, because the Au adatoms migrate freely on the surface, it is believed that the adsorption site of each adatom is different. Accordingly, the adatom-induced states may have different energy levels and wave function symmetry, which prevents the formation of an impuritylike band and the hybridization with the 2DEG band. Therefore, no band splitting is observed in Figs. 2(a)–2(d).

Because at 135 K, the Au adatoms are located on equivalent sites on the $\sqrt{3}$-Ag surface, the Au adatom

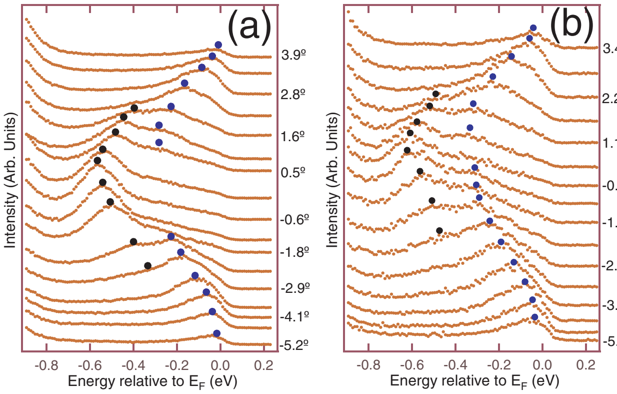

FIG. 3 (color online). ARPES results for the $\sqrt{3}$-Ag surface with small amounts (~ 0.03 ML) of (a) Ag and (b) Cs adatoms deposited at 135 K. The measurement conditions are the same as for the Au adatoms.

configuration is a subset of the $\sqrt{3}$-Ag crystalline configuration. Therefore, it is possible to include the Au adatom-induced resonant states in the same momentum set as that of the 2DEG band. Assuming the energy level of the resonant state to be E_a relative to E_F, the Hamiltonian for this 2D system would be

$$H = \sum_{\mathbf{k}\sigma} [\varepsilon_{\mathbf{k}} c^{\dagger}_{\mathbf{k}\sigma} c_{\mathbf{k}\sigma} + E_a a^{\dagger}_{\mathbf{k}\sigma} a_{\mathbf{k}\sigma} + V(a^{\dagger}_{\mathbf{k}\sigma} c_{\mathbf{k}\sigma} + c^{\dagger}_{\mathbf{k}\sigma} a_{\mathbf{k}\sigma})]. \qquad (2)$$

The first term describes the unperturbed 2DEG band $\varepsilon_{\mathbf{k}}$ with wave vector **k** and spin σ. The second term represents the electrons in the adatom-induced band at E_a. The third term accounts for the hybridization between these two bands, with energy V, set to be independent of **k** for simplicity. By diagonalizing this Hamiltonian, the hybridized energy dispersion is obtained to be

$$E_{\pm} = \frac{1}{2}(\varepsilon_{\mathbf{k}} + E_a) \pm \frac{1}{2}\sqrt{(\varepsilon_{\mathbf{k}} - E_a)^2 + 4V^2}. \qquad (3)$$

The unperturbed 2DEG band $\varepsilon_{\mathbf{k}}$ can be obtained from Figs. 2(a)–2(c) at RT where the hybridization effect is not yet seen, i.e., $\varepsilon_{\mathbf{k}} = E(\mathbf{k}_{\parallel})$. Then, using the parameters given in Table I for the corresponding Au coverage, Eq. (1) can be substituted into Eq. (3), which can then be used to fit the ARPES spectra taken at 135 K in Figs. 2(e)–2(g). The results are shown by solid lines that nicely reproduce the experimental measurements. The values of E_a and V used in the fit are listed in Table I. A general hybridization effect is schematically illustrated in the inset between Figs. 2(e) and 2(f). The conduction band ϵ_k and the localized virtual bound state E_a before hybridization are shown by dashed lines. After hybridization, the primary band ϵ_k is split by E_a into two bands, E_+ and E_-. It is noted that at large wave vectors the localized state E_a makes a dominant contribution to the band E_-. This is why the lower split band in our spectra becomes invisible at large wave vectors; the signal from the localized states become too weak.

We can see in Table I that both E_a and V are independent of the Au coverage within experimental uncertainty; i.e., the position of the impurity band is ~0.22 eV and the hybridization energy is ~0.11 eV. This is not unexpected considering that they are mainly determined by the attractive potential around the individual Au adatoms to the 2DEG electrons. An intuitive interpretation of the gap opening is that delocalized electrons at the energy level E_a are trapped in virtual bound states around the adatoms. In other words, E_a and V denote the energy level and size of the gap, respectively. On the other hand, it is known that at a Au coverage of 0.14 ML, the Au adatoms arrange themselves periodically to form a Si(111)$\sqrt{21} \times \sqrt{21}$-(Ag + Au) superstructure, and its 2DEG band has a gap opening at the $\sqrt{21} \times \sqrt{21}$ Brillouin zone boundary [17]. Interestingly, the energy gap at the zone boundary and that of the adatom-induced resonant state described here occur at a similar energy level (~0.25 eV and ~0.22 below the Fermi level, respectively), the size of the gap in the present study (~110 meV) is around twice that of the gap at the zone boundary (55 meV [17]). This implies that there is a strong relation between the resonant state and the 2DEG band of the $\sqrt{21} \times \sqrt{21}$-(Ag + Au) superstructure, though further studies are necessary to determine the transition from the impurity state to the continuum state.

To summarize, monovalent metal atoms adsorbed on a $\sqrt{3}$-Ag surface produce adatom-induced bound states that overlap, forming an impuritylike band at low temperature. This band hybridizes with the 2DEG band of the substrate, splitting it in two. To our knowledge, this is the first experimental evidence directly demonstrating such an interaction of bound electrons with delocalized electrons, resulting in a gap opening in a 2DEG band.

K. Kobayashi at Ochanomizu University is sincerely acknowledged for valuable discussions. This work was supported by a Grant-In-Aid from the Japanese Society for the Promotion of Science.

---

*Electronic address: liu@surface.phys.s.u-tokyo.ac.jp

[1] B. Simon, Ann. Phys. (N.Y.) **97**, 279 (1976).

[2] F.E. Olsson *et al.*, Phys. Rev. Lett. **93**, 206803 (2004).

[3] L. Limot, E. Pehlke, J. Kröger, and R. Berndt, Phys. Rev. Lett. **94**, 036805 (2005).

[4] T. Hirahara, I. Matsuda, M. Ueno, and S. Hasegawa, Surf. Sci. **563**, 191 (2004).

[5] S. Hasegawa, X. Tong, S. Takeda, N. Sato, and T. Nagao, Prog. Surf. Sci. **60**, 89 (1999).

[6] I. Matsuda *et al.*, Phys. Rev. B **71**, 235315 (2005).

[7] C. Liu, I. Matsuda, and S. Hasegawa, Surf. Interface Anal. **37**, 101 (2005).

[8] C. Liu, S. Yamazaki, R. Hobara, I. Matsuda, and S. Hasegawa, Phys. Rev. B **71**, 041310(R) (2005).

[9] N. Sato *et al.*, Phys. Rev. B **60**, 16 083 (1999).

[10] T. Nagao, K. Tsuchie, S. Hasegawa, and S. Ino, Phys. Rev. B **57**, 10 100 (1998).

[11] Y. Nakajima *et al.*, Phys. Rev. B **56**, 6782 (1997).

[12] In Fig. 2, except the S_1 band, only the edge of the S_2 band at ~ -0.8 eV is displayed in the dispersion images, which does not shift as the Au coverage increases.

[13] J.N. Crain, M.C. Gallagher, J.L. McChesney, M. Bissen, and F.J. Himpsel, Phys. Rev. B **72**, 045312 (2005).

[14] L. Chen, H.J. Xiang, B. Li, A. Zhao, X. Xiao, J. yang, J.G. Hou, and Q. Zhu, Phys. Rev. B **70**, 245431 (2004).

[15] J.H. Davies, *The Physics of Low-Dimensional Semiconductors* (Cambridge University Press, Cambridge, England, 1998).

[16] T. Ando, A.B. Fowler, and F. Stern, Rev. Mod. Phys. **54**, 437 (1982).

[17] J.N. Crain *et al.*, Phys. Rev. B **66**, 205302 (2002).